Biochemical and Biophysical Research Communications 403 (2010) 46–51

Contents lists available at ScienceDirect

Biochemical and Biophysical Research Communications

journal homepage: www.elsevier.com/locate/ybbrc

The role of active site residues in the oxidant specificity of the Orp1 thiol peroxidase ☆

Christina L. Takanishi, Li-Hua Ma, Matthew J. Wood *

Department of Environmental Toxicology, University of California, Davis, One Shields Ave, 4138 Meyer Hall, CA 95616, USA

ARTICLE INFO

Article history:
Received 20 October 2010
Available online 29 October 2010

Keywords:
Yap1
Sulfenic acid
Reactive oxygen species
tert-butyl-hydroperoxide
Cumene hydroperoxide
Oxidative stress

ABSTRACT

In this study we investigated the role of active site residues in the peroxidase activity of Orp1 (GPx3) using three different peroxide substrates. Using a structural homology model of the reduced form of Orp1, we identified Asn126 and Phe127 as evolutionarily conserved residues that line the back of the Orp1 active site and which are likely to affect the peroxidase activity of Orp1. Additionally, we identified Phe38 as a surface residue that could influence substrate specificity as it is located adjacent to Cys36, in the same position occupied by similar hydrophobic amino acids in many Orp1 homologs. We individually mutated these residues to alanine and examined the effect of each mutation *in vitro* and *in vivo*. Chloro-4-nitrobenzo-2-oxa-1,3-diazole was used to identify Cys-SOH modification of Cys36 in response to H_2O_2, *tert*-butyl-hydroperoxide (*tert*-BHP), and cumene hydroperoxide (CHP) in Orp1^{WT}. Mutation of Asn126 and Phe127 eliminate Cys-SOH formation and peroxidase activity in response to H_2O_2, *tert*-BHP and CHP. Furthermore, the pK_a of Cys36 is elevated closer to that of free cysteine compared to Orp1^{WT}. Mutation of Phe38 does not affect the peroxidase activity of Orp1 upon exposure to H_2O_2. The Phe38 mutation decreases Orp1 peroxidase activities in response to either *tert*-BHP or CHP. The *in vivo* sensitivity of the Phe38 mutant to both *tert*-BHP and CHP is increased, while the H_2O_2 sensitivity is unchanged. The pK_a of Cys36 in the Phe38 mutant is 5.0, which is the same as Orp1^{WT}. Taken together, these results suggest that Phe38 does not play a role in the reactivity of Cys36, but does modulate the affinity of Orp1 for alkyl hydroperoxides.

1. Introduction

The damage caused by reactive oxidative species (ROS) has been linked to a wide variety of human diseases such as atherosclerosis, Parkinson's disease, Alzheimer's disease, and cancer [1,2]. Therefore, the ability to sense and respond to a wide range of ROS is vital for the survival of all aerobic organisms. Intracellular ROS, such as hydrogen peroxide (H_2O_2) and alkyl hydroperoxides, occur naturally within cells, but also result from exposure to environmental contaminants such as cadmium and arsenic [3–6]. To counteract the damaging effects of ROS, the intracellular environment of the cell is maintained under reducing conditions in part by proteins that detoxify reactive oxidative species. Many of these proteins are involved in peroxide scavenging as well as the regulation of peroxide mediated signaling through complex redox-relay systems that have yet to be fully characterized [7].

Glutathione peroxidases (GPxs) form a large, phylogenetically conserved family of over 700 enzymes that utilize a peroxidatic cysteine (C_P) or selenocysteine (U_P) to reduce and thereby detoxify peroxides [8,9]. The three-dimensional environment surrounding C_P or U_P affect both its reactivity and accessibility. The Orp1 thiol peroxidase is homologous to glutathione peroxidases and plays a dual role in the oxidative stress response pathway in *S. cerevisiae*. It detoxifies both H_2O_2 and alkyl hydroperoxides, such as *tert*-butyl-hydroperoxide (*tert*-BHP) and cumene hydroperoxide (CHP), and mediates the oxidative stress response in concert with the Yap1 transcription factor [10,11]. The C_P (Cys36) on Orp1 has been shown to form a cysteine sulfenic acid (Cys-SOH) intermediate upon exposure to H_2O_2 [12]. The Cys-SOH intermediate either forms an intramolecular disulfide bond with resolving cysteine (Cys82), which is reduced by thioredoxin, or an intermolecular disulfide bond with Cys598 on Yap1, leading to its activation [10,11]. In Orp1, the residues Gln70 and Trp125 form the catalytic triad with Cys36. Mutation of Gln70 or Trp125 to alanine removes the ability of Cys36 to form Cys-SOH and increases the pK_a of Cys36 from 5.1 to 8.3 [12]. This work investigates the role of residues surrounding the Orp1 active site in moderating its peroxide reactivity.

☆ This work was funded by a grant from the American Heart Association (0635328N).

* Corresponding author. Fax: +1 530 752 3394.
E-mail address: mjwood@ucdavis.edu (M.J. Wood).

0006-291X/$ - see front matter © 2010 Elsevier Inc. All rights reserved.
doi:10.1016/j.bbrc.2010.10.109

2. Materials and methods

2.1. Chemicals

Chloro-4-nitrobenzo-2-oxa-1,3-diazole (NBD-Cl), β-NADPH, *tert*-BHP and iodoacetamide, were purchased from Sigma–Aldrich. Thioredoxin reductase (*Escherichia coli* recombinant, lyophilized powder) was purchased from CalBiochem. Dithiothreitol (DTT), H_2O_2, and cumene hydroperoxide (CHP) were purchased from Fisher. (2-pyridyl)-dithiobimane (PDT-Bimane) was purchased from Toronto Research Biochemicals.

2.2. Homology model of Orp1

The three-dimensional model of reduced Orp1 was calculated based on the X-ray crystal structures of human hGPx2 (PDB code 2HE3) and hGPx5 (PBD code 2I3Y) as previously described [12].

2.3. Protein cloning, expression, and purification

The *ORP1* gene was cloned from *S. cerevisiae* genomic DNA, subcloned into the pRSET vector, and purified as described previously [12,13]. Orp1 single and double point mutants were made using standard PCR-based mutagenesis. The Yap1-cCRD protein was designed and purified as described previously [14].

2.4. Homology model of Orp1, detection of cysteine sulfenic acid modifications with NBD-Cl, pK_a determination of Orp1 sulfhydryls with PDT-Bimane

Experiments were carried out as previously described [12].

2.5. Enzyme activity assay

The decrease in absorbance of NADPH was used to indirectly measure peroxidase activity of Orp1 *in vitro*. 1.35 μM of purified wild-type Orp1 or mutant Orp1 was mixed with 1.35 μM TrxA, 1.44 μM TrxB, and 300 μM β-NADPH in a total volume of 100 μL in a buffer containing 100 mM Tris (pH 8.0) and 10 mM EDTA and incubated at 25 °C for 10 min. One hundred μM of peroxide (H_2O_2, CHP, or *tert*-BHP) in 1 μL was added to start the reaction and the absorbance of NADPH at 340 nm was measured every 15 s for 5 min. The results were baseline corrected and normalized using the absorbance from a reaction containing all components except peroxide.

2.6. Analysis of Orp1 mutations in vivo

In vivo analysis was carried out as previously described [12]. Yeast were normalized for cell number and serial dilutions were spotted onto freshly prepared YPD plates with 0, 0.75, 1.5, and 2.25 mM H_2O_2, 0, 0.05, 0.10, and 0.15 mM CHP, or 0, 0.15, 0.30, 0.45, and 0.60 mM *tert*-BHP and incubated at 30 °C for 2 days.

3. Results

3.1. Identification of Orp1 active site residues that modulate redox activity

The amino acid sequence of Orp1 is highly conserved among other members of the GPx family. Fig. 1A presents a protein sequence alignment of seven homologous proteins. Orp1 Cys36 is conserved in all aligned proteins. We hypothesized that conserved residues in structural proximity to Cys36 influence the peroxidase activity of Orp1 and would therefore have the greatest effect when mutated. To identify candidate residues, we used a homology model of reduced Orp1 based on the X-ray crystallographic structures of hGPx2 and hGPx5 (Fig. 1B). We identified Phe38, Asn126 and Phe127 as residues that would likely play a role in Orp1 redox activity. Phe38 and Phe127 are located within 4.20 and 3.07 Å, respectively, of Cys36, while the carboxamide group of Asn126 is located 4.47 Å away from Cys36. Both Asn126 and Phe127 are strictly conserved in Orp1 homologs (Fig. 1A). Conversely, Phe38 is conserved in only three of the seven Orp1 homologs. In the remaining three, this position is occupied by a leucine. The proximity to Cys36, coupled with its hydrophobicity and position on the surface of Orp1, indicate that Phe38 might play a role in Orp1 reactivity with peroxides such as *tert*-BHP and CHP.

3.2. Mutational analysis of Orp1 peroxidase activity

To determine if Phe38, Asn126 and Phe127 are required for the peroxidase activity of Orp1, we purified wild-type Orp1 and Orp1 containing point mutations of Phe38 to Ala ($Orp1^{F38A}$), Asn126 to Ala ($Orp1^{N126A}$), and Phe127 to Ala ($Orp1^{F127A}$) for use in peroxidase activity assays. For these assays, enzyme activity was measured using a spectrophotometric assay that indirectly measures the ability of Orp1 to reduce peroxides via a decrease in absorbance of NADPH at 340 nm [15]. Orp1 was mixed with *b*TrxA, *b*TrxB, and NADPH and the reaction was initiated with the addition of 100 μM H_2O_2, *tert*-BHP, or CHP. The rate of enzyme activity, was similar for wild-type Orp1 upon exposure to H_2O_2 or *tert*-BHP, but was decreased for CHP (Fig. 2A). $Orp1^{F38A}$ showed slightly decreased peroxidase activity compared to WT Orp1 upon addition of *tert*-BHP, and CHP (Fig. 2B). In contrast, both $Orp1^{N126A}$ and $Orp1^{F127A}$ showed a dramatic loss of peroxidase activity for all three peroxides (Fig. 2C and D).

3.3. Characterization of Cys36 sulfenic acid formation in response to peroxides

To further characterize the $Orp1^{F38A}$, $Orp1^{N126A}$ and $Orp1^{F127A}$ mutations, we monitored the formation of Cys-SOH on Cys36. We used the chemical 7-chloro-4-nitrobenzo-2-oxa-1,3-diazole (NBD-Cl) to probe for Cys-SOH modification of Cys36 in response to upon addition of H_2O_2, *tert*-BHP, and CHP [15]. We have previously shown that the Orp1 active site Cys36 forms Cys-SOH in response to H_2O_2 [12]. To determine if the mutation of residues Phe38, Asn126, or Phe127 affect the formation of Cys-SOH on Cys36, we used a previously characterized Orp1 mutant in which Cys64 and Cys82 were mutated to serine ($Orp1^{C36}$). We subsequently mutated Phe38 to Ala ($Orp1^{C36/F38A}$), Asn126 to Ala ($Orp1^{C36/N126A}$), and Phe127 to Ala ($Orp1^{C36/F127A}$).

We treated $Orp1^{C36}$ with H_2O_2, *tert*-BHP, or CHP before the addition of NBD-Cl. As a negative control $Orp1^{C36}$ was reacted with NBD-Cl alone. Unreacted NBD-Cl was removed from all solutions by gel filtration chromatography and protein samples were concentrated prior to UV–visible spectroscopy. Fig. 3A shows the spectra of $Orp1^{C36}$. The $Orp1^{C36}$ protein alone shows a peak with a maximal absorbance at 280 nm, while the spectrum of $Orp1^{C36}$ combined with NBD-Cl shows an additional peak with a maximal absorbance at 420 nm. The presence of a peak at 420 nm is indicative of the reaction of NBD-Cl with the sulfhydryl form of Cys36 (R-S-NBD). The reaction of NBD-Cl and $Orp1^{C36}$ in the presence of H_2O_2, *tert*-BHP, or CHP all show peaks with maximal absorbance at 347 nm (Fig. 3A). The presence of the 347 nm peak is indicative of Cys-SOH formation on Cys36 (R-SO-NBD). The results for *tert*-BHP and CHP are consistent with previous results obtained with $Orp1^{C36}$. The reaction of NBD-Cl with $Orp1^{C36/F38A}$ after addition of H_2O_2 results in a similar spectrum as that of $Orp1^{C36}$ (Fig. 3B). This spectrum

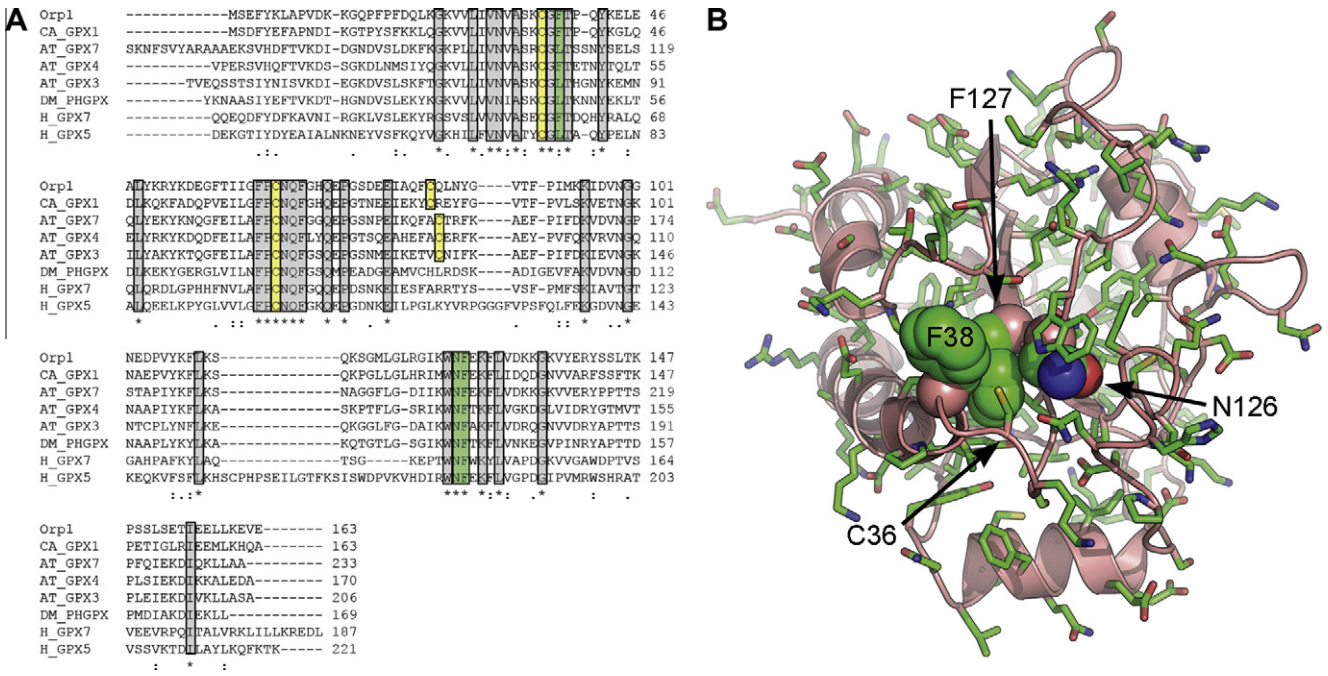

Fig. 1. Orp1 active site model. (A) Primary sequence alignment of homologous proteins *Candida albicans* GPx1, *Arabidopsis thaliana* GPx7, GPx4, and GPx3, *Drosophila melanogaster* PHGPx, and human GPx7 and GPx5. Conserved cysteine residues are highlighted in yellow. Conserved residues of interest are highlighted in green. All other conserved amino acids are highlighted in grey. (B) A three-dimensional model of Orp1 shows Cys36 (stick) in close proximity to surrounding key residues (space-filled) in the active site. Phe38 and Phe127 line the hydrophobic left side of the pocket, while Asn126 lines the polar right side of the pocket. (For interpretation of the references to colour in this figure legend, the reader is referred to the web version of this article.)

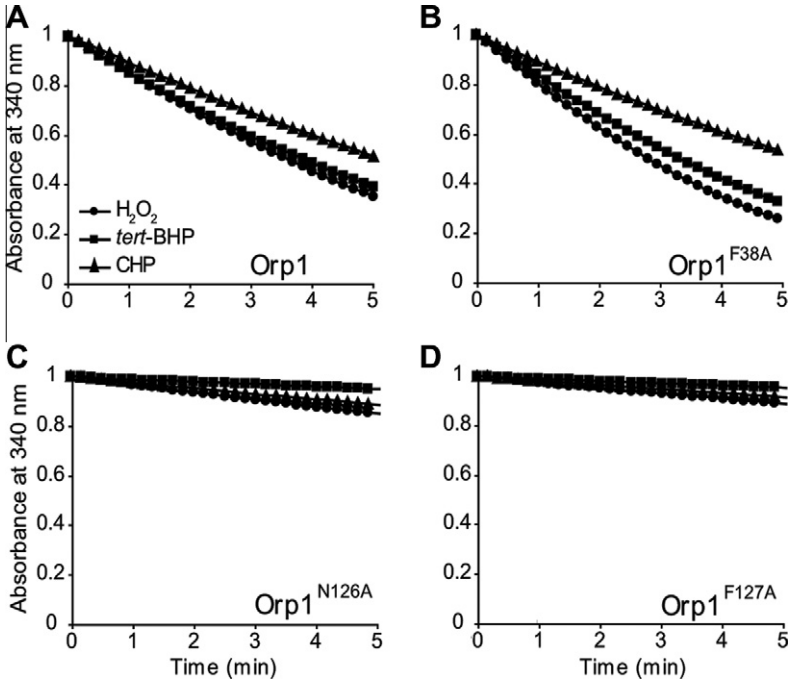

Fig. 2. Orp1 peroxidase activity varies between mutants. Orp1 was exposed to 100 μM H_2O_2, *tert*-BHP, or CHP and Orp1 peroxidase activity was measured using an NADPH-coupled assay. The absorbance of NADPH was measured at 340 nm. The activity for wild-type Orp1 (A), $Orp1^{F38A}$ (B), $Orp1^{N126A}$ (C), and $Orp1^{F127A}$ (D) is shown for all three peroxides.

has a peak at 347 nm indicating the formation of Cys-SOH on Cys36. In contrast to H_2O_2-treated $Orp1^{C36/F38A}$, treatment with *tert*-BHP results in a decrease in the intensity of the 347 nm peak and an increase in the 420 nm peak, suggesting that Cys-SOH formation is decreased in response to *tert*-BHP (Fig. 3B). Treatment with CHP results in a slight decrease in absorbance at 347 nm, compared to wild-type. Finally, the reaction of NBD-Cl and $Orp1^{C36/N126A}$ or $Orp1^{C36/F127A}$ in the presence of H_2O_2, *tert*-BHP, or CHP shows only one peak at 420 nm, suggesting that Cys-SOH was not formed on Cys36 in these Orp1 mutants (Fig. 3C and D).

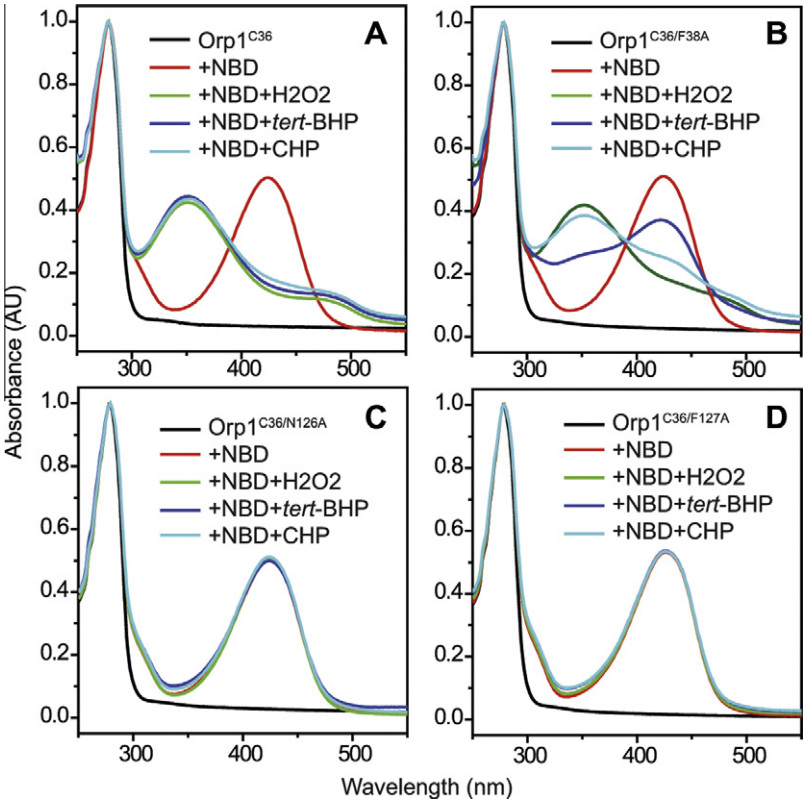

Fig. 3. Sulfenic acid formation differs between mutants. NBD-Cl was used to test for the ability of Orp1 to form sulfenic acid in response to various peroxides. When reacted with NBD-Cl, the wild-type Orp1 spectra show a peak at 347 nm (R-S(O)NBD) for H_2O_2, *tert*-BHP, and CHP (A). The $Orp1^{F38A}$ spectra show a peak at 347 nm for H_2O_2 and CHP and a peak at 420 nm (R-S-NBD) for *tert*-BHP (B). The $Orp1^{N126A}$ (C) and $Orp1^{F127A}$ (D) spectra show peaks at 420 nm.

3.4. pK_a determination of the Orp1 thiols

The pK_a of a cysteine residue is a measure of its propensity to exist as a deprotonated thiolate anion. Since the thiolate has enhanced nucleophilicity when compared to the parent thiol, cysteine pK_a directly impacts its reactivity with other molecules. Reactive cysteines known to form Cys-SOH have a pK_a lower than that of free cysteine and are found in proteins such as the cysteine protease papain (pK_a = ~4) [16] and *Salmonella typhimurium* AhpC (pK_a = 5.9) [24]. The pK_a of Cys36 on Orp1 was previously determined to be 5.1 using an assay involving chemical modification by PDT-Bimane [17]. The reaction of PDT-Bimane with cysteine forms pyridine-2-thione, which has a maximum absorption wavelength of 343 nm. When measured over time, this reaction spectrum can be fit to a first order exponential function to determine a t_1 value. Reactions using PDT-Bimane were conducted with $Orp1^{C36/F38A}$, $Orp1^{C36/N126A}$, and $Orp1^{C36/F127A}$ over a range of pH values, from 3.5 to 11.0. The t_1 values were normalized and plotted as a function of pH (Fig. 4A) and the points were fit to the Henderson–Hasselbach equation to determine the pK_a of Cys36. The pK_a of the $Orp1^{C36/F38A}$ mutant was found to be 5.0, very close to that of wild-type Orp1 (5.1). Similar to previous observations with mutants containing alanine in place of Gln70 or Trp125, the pK_a values determined for mutants containing alanine in place of Asn126 or Phe127 were elevated to 8.6 and 8.3, respectively, closer to that of free cysteine. These data suggest that Asn126 and Phe127 are involved in the stabilization of Cys36 in its thiolate form and modulating its general reactivity.

3.5. Analysis of Orp1 mutations in vivo

For Orp1 containing the Phe38 to Ala mutation, the enzyme activity, Cys-SOH formation, and complex formation with Yap1-cCRD differed from that of wild-type Orp1 in a peroxide dependent manner. Both $Orp1^{C36/F38A}$ and $Orp1^{F38A}$ were able to react normally with H_2O_2, but had impaired reactivity with *tert*-BHP and CHP. To better understand the role of Phe38 in Orp1 peroxide reactivity, we characterized the phenotype of the $Orp1^{F38A}$ *S. cerevisiae* mutant in response to various peroxides. To accomplish this, we transformed a Δ*orp1 S. cerevisiae* strain with integrating plasmids containing wild-type *orp1*, $orp1^{F38A}$, or ppp81 as a vector control. The resulting strains were tested for their ability to form colonies in the presence of peroxide. The parental strain, YPH499, was used as the positive control. All strains were spotted onto plates containing increasing amounts of H_2O_2, *tert*-BHP, or CHP. The wild-type strain was able to grow on plates containing up to 2.25 mM H_2O_2, 0.6 mM *tert*-BHP, or 0.15 mM CHP, while the Δ*orp1* strain showed a significant decrease in colony forming ability (Fig. 4B). This highlights the crucial role of Orp1 for yeast survival upon exposure to hydroperoxides. Yeast transformed with the empty vector showed the same phenotype as the Δ*orp1* strain. The phenotype of yeast containing wild-type Orp1 was restored to that of the parental wild-type strain YPH499. The strain containing $Orp1^{F38A}$ grew similar to YPH499 in response to H_2O_2 (Fig. 4B). In contrast, and consistent with our *in vitro* assays, $Orp1^{F38A}$ has diminished colony forming ability compared to wild-type Orp1 at concentrations of *tert*-BHP and CHP approaching 0.6 and 0.15 mM, respectively.

4. Discussion

In this study we characterized the role of Orp1 active site residues in peroxide reactivity and redox-mediated signal transduction. We observed Cys-SOH formation on Cys36 of Orp1 in response to the alkyl hydroperoxides *tert*-BHP and CHP. We used a structural model of reduced Orp1 derived from the crystal

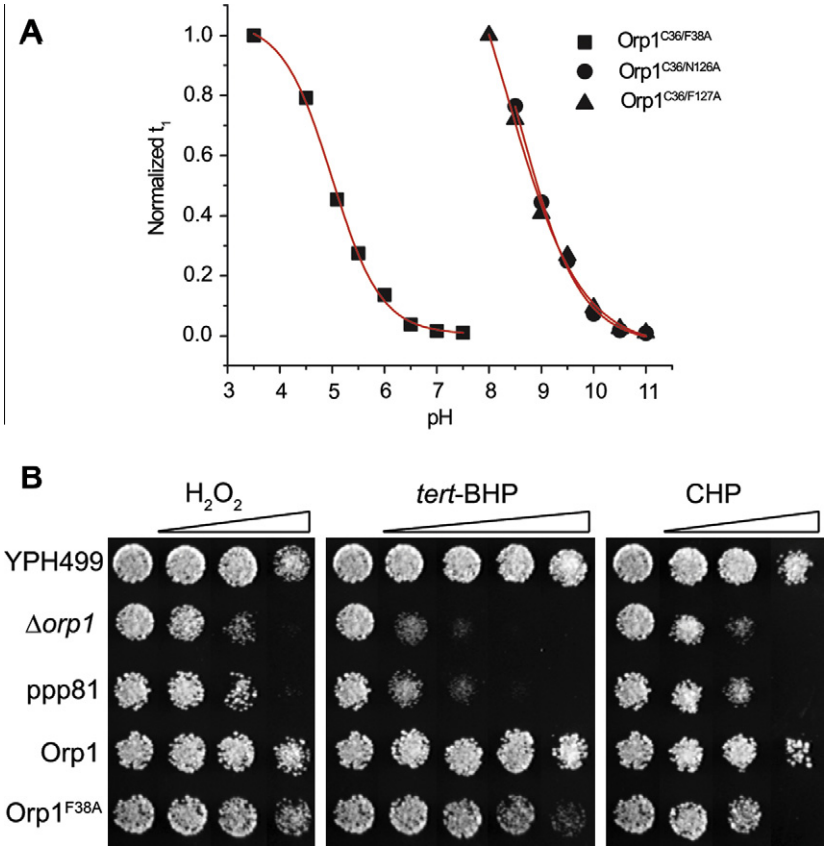

Fig. 4. Analysis of Orp1 mutants. (A) Reactions of Orp1$^{C36/F38A}$, Orp1$^{C36/N126A}$, or Orp1$^{C36/F127A}$ with PDT-Bimane were monitored at 343 nm at pH values ranging from 4.0 to 7.5 or 8.0 to 11.0. First order rate constants (t_1) were determined and plotted as a function of pH. The results were fit to Henderson–Hasselbach equation and sulfhydryl pK_a values of 5.0, 8.6, and 8.3 were determined for the Orp1^{C36}, Orp1$^{C36/F38A}$, Orp1$^{C36/N126A}$ and Orp1$^{C36/F127A}$, respectively. (B) H_2O_2, *tert*-BHP, and CHP resistance phenotypes of the parental *S. cerevisiae* strain (YPH499), Orp1 deletion (Δ*orp1*), empty ADH1 integrating vector (ppp81), ADH1 integrated Orp1, and Orp1^{F38A} are shown. Both YPH499 and ADH1 integrated Orp1 were able to form colonies out to 2.25 mM H_2O_2, 0.6 mM *tert*-BHP, and 0.15 mM CHP. Orp1^{F38A} showed a phenotype similar to wild-type Orp1 when exposed to H_2O_2, but was not as resistant as wild-type Orp1 when exposed to *tert*-BHP or CHP.

structures of hGPx enzymes to discover residues that could potentially modulate the reactivity of Cys36. Mutation of conserved residues Asn126 or Phe127 to alanine resulted in the loss of Orp1 peroxidase activity, loss of Cys-SOH formation on Cys36, and a notable increase in the pK_a of Cys36 compared to wild-type. Similar results were observed in Orp1 Gln70 and Trp125 mutants [12]. The Orp1^{F38A} mutant responded similar to wild-type when exposed to H_2O_2 and retains the ability to form Cys-SOH on Cys36 in response to H_2O_2. Though the pK_a of Cys36 in Orp1^{F38A} was unaffected, there was a decrease in Cys-SOH formation in response to *tert*-BHP or CHP, suggesting that Phe38 is not involved in the catalytic activity of Orp1, but influences peroxide specificity, which alters the ability of Orp1 to act as an alkyl hydroperoxidase.

The results of our initial mutational studies of Asn126 and Phe127 were similar to the results of studies involving mutations of Gln70 or Trp125, which show that these residues decrease the pK_a of Cys36 and are necessary for Orp1 peroxidase activity in response to all peroxides tested. Asn126 in *S. cerevisiae* is homologous to Asn136 in *D. melanogaster*, previously described as the 4th member of the catalytic triad [18]. The finding that the F38A mutation leads to the decreased ability to grow in the presence of alkyl hydroperoxides, but not H_2O_2, raises interesting questions about Orp1 peroxide specificity. Our model of Orp1 shows Phe38 on the surface of Orp1 near Cys36. Mutation of this residue to alanine removes the large benzyl side chain on the surface of the protein, which may decrease Van der Waals interactions and eliminate possible ring stacking with other aromatic compounds, such as CHP. The benzyl side chain may also affect the steric conformation of the active site pocket to alter the binding of larger hydroperoxides. Phe38 is partially conserved among GPxs, while other members of the GPx family contain a leucine in the corresponding position. These bulky, hydrophobic amino acids may work to increase substrate specificity for hydrophobic hydroperoxides, while, simultaneously, maintaining the affinity for hydrogen peroxide. Further evidence for the role of Phe38 in Orp1 substrate specificity would be provided by structural data showing Orp1-substrate complexes.

In contrast to Phe38, Asn126, and Phe127 are found in the interior of the active site of Orp1. These mutations likely affect different aspects of Cys36 reactivity. Phe127 does not have the ability to contribute to the hydrogen bonding network in the active site, and thus does not directly contribute to the lowered pK_a of Cys36. It does lie directly behind Cys36 and the bulky aromatic side chain could provide structure to the surrounding residues in the active site. The mutation of Phe127 to alanine likely results in the collapse of the active site and decoupling of the catalytic triad. Asn126 is located between Trp125 and Gln70 and its carboxamide group points directly at Cys36. As suggested for Asn136 and Gln 80 in *D. melanogaster*, coordination of the carboxamide groups on Asn126 and Gln70 with the thiol group on Cys increases the reactivity of the C_P, with Asn126 aiding in activation of C_P, allowing for polarization of the hydroperoxide by Gln to facilitate its cleavage [18].

Our homology mode, which is based on hGPx enzyme structures, aligns well with the X-ray crystal structure of *Bos taurus* GPx1 (*Bt*GPx1, PDB code 1GP1). The partial X-ray crystal structure

of what appears to be oxidized Orp1, was also recently published (called Hyr1, PDB code 3CMI) [19]. Our model is very close to that of the Orp1 crystal structure, with the main difference in the position of the Cys36 residue. The Hyr1 structure shows Cys36 facing out and away from the active site residue, too far for hydrogen bonding to occur between the members of the catalytic triad. As noted in a previous publication, the active site cysteine Cys36 is approximately 10 Å away from the resolving cysteine Cys82, suggesting that the loop containing Cys82 is flexible. The published Hyr1 structure was crystallized under conditions lacking reducing agent and therefore likely represents the Cys36–Cys82 disulfide bonded form of Orp1. Superimposition of the Hyr1 structure onto *Bt*GPx1 shows Cys36 in close proximity to the α-helix of *Bt*GPx1, where the resolving Cys82 on Orp1 would be. We suggest that the Cys36-containing loop of Orp1 is flexible and that the reactive cysteine is able to move in and out of the active site pocket, depending on the redox state of the protein, and that our model likely represents the reduced form of Orp1.

In the mammalian catalytic triad, it is known that hydrogen bonding between the imino group of the active site Trp residue and the amido group of the active site Gln residue stabilizes the selenol group and increases the reactivity of the active site selenocysteine towards hydroperoxides [20]. Increasing evidence has shown that residues that alter the reactivity of C_P are not limited to those in the catalytic triad. It has been reported that in the serine protease subtilisin replacement of the catalytic serine residue with a selenocysteine residue changes the protease into a peroxidase and that interactions between selenocysteine and neighboring His and Asp residues give selenosubtilisin its efficient peroxidase activity [21]. Molecular modeling has also demonstrated the existence of a catalytic triad in human TrxR involving Cys, His, and Glu and subsequently Sec, His, and Glu [22]. These examples highlight the importance of the interactions between the active site Cys or Sec and surrounding residues.

The ability to differentiate between classes of hydroperoxides influences peroxidase activity as well as cellular signaling of GPxs and related peroxiredoxins. For example, *Salmonella typhimurium* AhpC is a peroxiredoxin shown to have a substrate preference for small peroxides, such as H_2O_2, over tertiary hydroperoxides [23]. This preference may help *St*AhpC regulate peroxide signaling through its over oxidation and inactivation in response to large amounts of H_2O_2 and maintenance of its activity in response to equivalent amounts of *tert*-BHP or CHP. As with peroxide scavenging proteins and peroxiredoxins, such as AhpC, reactivity of C_P and substrate specificity of the active site are important for defining the physiological role of Orp1 and other members of the GPx family. Certain residues, such as Asn126 and Phe127 play a role in the stability of active site cysteines, while residues such as Phe38, may not directly affect the reactivity of the C_P, but serve to modulate the substrate specificity of the active site.

Acknowledgments

We kindly thank Heather Bolstad and Nicholas Kettenhofen for insightful comments.

References

[1] B. Halliwell, The role of oxygen radicals in human disease, with particular reference to the vascular system, Haemostasis 23 (Suppl. 1) (1993) 118–126.
[2] N. Hogg, Free radicals in disease, Semin. Reprod. Endocrinol. 16 (1998) 241–248.
[3] M. Giorgio, M. Trinei, E. Migliaccio, P.G. Pelicci, Hydrogen peroxide: a metabolic by-product or a common mediator of ageing signals? Nat. Rev. Mol. Cell Biol. 8 (2007) 722–728.
[4] R. Takeya, H. Sumimoto, Regulation of novel superoxide-producing NAD(P)H oxidases, Antioxid. Redox Signal. 8 (2006) 1523–1532.
[5] E. Lopez, C. Arce, M.J. Oset-Gasque, S. Canadas, M.P. Gonzalez, Cadmium induces reactive oxygen species generation and lipid peroxidation in cortical neurons in culture, Free Radic. Biol. Med. 40 (2006) 940–951.
[6] H. Shi, X. Shi, K.J. Liu, Oxidative mechanism of arsenic toxicity and carcinogenesis, Mol. Cell Biochem. 255 (2004) 67–78.
[7] E.A. Veal, A.M. Day, B.A. Morgan, Hydrogen peroxide sensing and signaling, Mol. Cell 26 (2007) 1–14.
[8] S. Toppo, S. Vanin, V. Bosello, S.C. Tosatto, Evolutionary and structural insights into the multifaceted glutathione peroxidase (Gpx) superfamily, Antioxid. Redox Signal. 10 (2008) 1501–1514.
[9] R. Brigelius-Flohe, Glutathione peroxidases and redox-regulated transcription factors, Biol. Chem. 387 (2006) 1329–1335.
[10] A. Delaunay, D. Pflieger, M.B. Barrault, J. Vinh, M.B. Toledano, A thiol peroxidase is an H_2O_2 receptor and redox-transducer in gene activation, Cell 111 (2002) 471–481.
[11] M.J. Wood, G. Storz, N. Tjandra, Structural basis for redox regulation of Yap1 transcription factor localization, Nature 430 (2004) 917–921.
[12] L.H. Ma, C.L. Takanishi, M.J. Wood, Molecular mechanism of oxidative stress perception by the Orp1 protein, J. Biol. Chem. 282 (2007) 31429–31436.
[13] J.T. Mason, S.K. Kim, D.B. Knaff, M.J. Wood, Thermodynamic basis for redox regulation of the Yap1 signal transduction pathway, Biochemistry 45 (2006) 13409–13417.
[14] C.L. Takanishi, L.H. Ma, M.J. Wood, A genetically encoded probe for cysteine sulfenic acid protein modification in vivo, Biochemistry 46 (2007) 14725–14732.
[15] H.R. Ellis, L.B. Poole, Roles for the two cysteine residues of AhpC in catalysis of peroxide reduction by alkyl hydroperoxide reductase from Salmonella typhimurium, Biochemistry 36 (1997) 13349–13356.
[16] S. Pinitglang, A.B. Watts, M. Patel, J.D. Reid, M.A. Noble, S. Gul, A. Bokth, A. Naeem, H. Patel, E.W. Thomas, S.K. Sreedharan, C. Verma, K. Brocklehurst, A classical enzyme active center motif lacks catalytic competence until modulated electrostatically, Biochemistry 36 (1997) 9968–9982.
[17] S.E. Mansoor, D.L. Farrens, High-throughput protein structural analysis using site-directed fluorescence labeling and the bimane derivative (2-pyridyl)dithiobimane, Biochemistry 43 (2004) 9426–9438.
[18] S.C. Tosatto, V. Bosello, F. Fogolari, P. Mauri, A. Roveri, S. Toppo, L. Flohe, F. Ursini, M. Maiorino, The catalytic site of glutathione peroxidases, Antioxid. Redox Signal. 10 (2008) 1515–1526.
[19] W.J. Zhang, Y.X. He, Z. Yang, J. Yu, Y. Chen, C.Z. Zhou, Crystal structure of glutathione-dependent phospholipid peroxidase Hyr1 from the yeast Saccharomyces cerevisiae, Proteins 73 (2008) 1058–1062.
[20] O. Epp, R. Ladenstein, A. Wendel, The refined structure of the selenoenzyme glutathione peroxidase at 0.2-nm resolution, Eur. J. Biochem. 133 (1983) 51–69.
[21] R. Syed, Z.P. Wu, J.M. Hogle, D. Hilvert, Crystal structure of selenosubtilisin at 2.0-A resolution, Biochemistry 32 (1993) 6157–6164.
[22] S. Gromer, L.A. Wessjohann, J. Eubel, W. Brandt, Mutational studies confirm the catalytic triad in the human selenoenzyme thioredoxin reductase predicted by molecular modeling, Chembiochem 7 (2006) 1649–1652.
[23] D. Parsonage, P.A. Karplus, L.B. Poole, Substrate specificity and redox potential of AhpC, a bacterial peroxiredoxin, Proc. Natl. Acad. Sci. USA (2007) 8209–8214.
[24] K.J. Nelson, D. Parsonage, A. Hall, P.A. Karplus, L.B. Poole, Cysteine pK(a) values for the bacterial peroxiredoxin AhpC. Biochemistry 47 (2008) 12860–12868.